Modulation of the boreal wintertime Madden-Julian oscillation by the stratospheric quasi-biennial oscillation

Changhyun Yoo[1] and Seok-Woo Son[2]

[1]Department of Atmospheric Science and Engineering, Ewha Womans University, Seoul, South Korea, [2]School of Earth and Environmental Sciences, Seoul National University, Seoul, South Korea

Abstract Madden-Julian oscillation (MJO), the dominant mode of intraseasonal variability in the tropical troposphere, has a significant impact on global weather and climate. Here we present that the year-to-year variation of the MJO activity shows significant changes with the quasi-biennial oscillation (QBO) in the tropical stratosphere. Specifically, the boreal winter MJO amplitude, evaluated by various metrics, is typically stronger than normal during the QBO easterly phase at 50 hPa and weaker than normal during the QBO westerly phase at 50 hPa. This relationship, which is possibly mediated by the QBO-related static stability and/or vertical wind shear changes in the tropical upper troposphere and lower stratosphere, is robust whether or not the activeness of the MJO or QBO is taken into account. This result suggests a new potential route from the stratosphere that regulates the organized tropical convection, helping to improve the prediction skill of the boreal winter MJO.

1. Introduction

The zonal mean zonal wind in the tropical stratosphere changes its sign approximately every other year (Figure 1a). This phenomenon, the so-called quasi-biennial oscillation (QBO), is the most prominent interannual variability in the stratosphere [*Baldwin et al.*, 2001]. Previous studies have demonstrated that the impact of the QBO is not limited to the stratosphere but reaches the troposphere [*Gray et al.*, 1992; *Giorgetta et al.*, 1999; *Garfinkel and Hartmann*, 2011]. In particular, it is reported that the QBO can affect the seasonal mean tropical convection [*Collimore et al.*, 2003] and the associated tropical-extratropical teleconnection [*Garfinkel and Hartmann*, 2011]. For instance, monsoonal precipitation over India weakens during the easterly phase of the QBO (EQBO) at 50 hPa, while the opposite is true during the westerly phase (WQBO) [*Kane*, 1995; *Giorgetta et al.*, 1999; *Claud and Terray*, 2007]. Deep convection over the western and central tropical Pacific has also been shown to be related to QBO phase in both observations [*Gray et al.*, 1992; *Collimore et al.*, 2003; *Huang et al.*, 2012] and numerical model experiments [*Giorgetta et al.*, 1999].

Motivated by these studies, we ask whether the QBO can make a significant impact on the interannual variation of the organized tropical convections that are associated with the Madden-Julian oscillation (MJO). It is well known that the MJO is the largest contributor to tropical convective variability at time scales of 30–90 days, which includes planetary-scale atmospheric circulations, moisture, and deep convections, propagating eastward from the Indian to Pacific Oceans [e.g., *Madden and Julian*, 1994]. Due to its extensive influence on global weather and climate [e.g., *Zhang*, 2014], as well as its importance for subseasonal to seasonal predictions [e.g., *Waliser et al.*, 2003], many efforts have been made to better understand the dynamics of the MJO and to improve the MJO prediction skill in the numerical models [*Miura et al.*, 2007; *Gottschalck et al.*, 2010; *Miyakawa et al.*, 2014].

Although the MJO itself is organized at the intraseasonal time scale, it undergoes significant seasonal and interannual variations caused by the mean flow changes [e.g., *Lau and Waliser*, 2005] (see also Figure 1b). Concerning interannual variation, internal variability of the MJO has been observed to play an important role [*Slingo et al.*, 1999]. In addition, a possible connection to the El Niño/Southern Oscillation (ENSO; Figure 1c), a dominant source of interannual variability in the tropical troposphere and the ocean, has previously been explored [*Hendon et al.*, 1999; *Slingo et al.*, 1999; *Hendon et al.*, 2007]. Despite some reports of MJO activity changes during different ENSO phases [*Gushchina and Dewitte*, 2012; *Feng et al.*, 2015], an ENSO-MJO link is still not well established [*Lin et al.*, 2015]. Apart from an association with sudden stratospheric warming [*Garfinkel et al.*, 2012; *Liu et al.*, 2014; *Albers et al.*, 2016], there has been little work linking the MJO to stratospheric variability, especially to the QBO [*Liu et al.*, 2014].
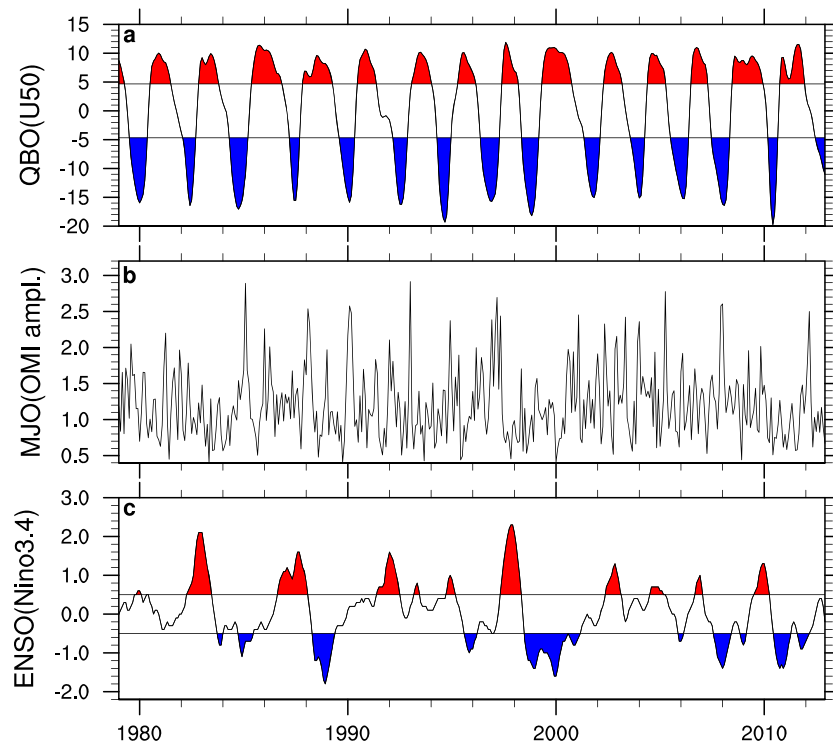
Figure 1. Time series of QBO index (U50), MJO amplitude, and ENSO index from 1979 to 2012 are shown. (a) The U50 is defined by 3 month moving averaged zonal mean zonal wind anomaly at 50 hPa, integrated over 10°S–10°N. WQBO (EQBO) phases, when U50 is greater (less) than the half of its standard deviation, are shaded in red (blue). (b) The MJO amplitude is measured by the amplitude of the OLR-based MJO index (OMI), which is first averaged for each month and then is smoothed by 3 month running mean. (c) For the ENSO index, monthly sea surface temperature (SST) anomalies, where the anomalies are deviations from the monthly climatology, are averaged for Niño 3.4 area (170°W–120°W, 5°S–5°N) and then are 3 month moving averaged. Values greater (less) than 0.5°C are shaded in red (blue).

2. Data and Methods

2.1. QBO Index

The monthly mean Interim European Center for Medium-Range Weather Forecasts Reanalysis (ERA-Interim) data set [*Dee et al.*, 2011] is used for the period from 1979 to 2012. The season of our primary interest is the boreal winter (i.e., December–February (DJF)), but we have also examined all other seasons. An index of the QBO is obtained using the 3 month running averaged monthly zonal mean zonal wind anomaly at 50 hPa (U50), integrated over 10°S–10°N, where the anomaly is obtained as a deviation from monthly climatology. The WQBO is defined when U50 is greater than half of its standard deviation (red shading in Figure 1a). Likewise, EQBO is defined when U50 is less than half of its standard deviation (blue shading in Figure 1a). Because QBO-related zonal wind anomalies propagate from the upper to the lower stratosphere [*Baldwin et al.*, 2001], the zonal mean zonal wind anomalies at different pressure levels (i.e., 10, 20, 30, and 70 hPa) are similarly indexed to examine the correlations between the QBO and the MJO (Table 1).

Table 1. Correlations Between Seasonally Averaged OMI Amplitude and Various QBO Indices[a]

	DJF	DJF-	NDJFM	MAM	JJA	SON
U70	**−0.56***	**−0.64**	**−0.49**	−0.27	0.10	0.13
U50	**−0.59***	**−0.61***	**−0.49**	−0.09	−0.09	0.10
U30	−0.17	−0.08	−0.12	0.19	**−0.23**	−0.03
U20	**0.33**	**0.53**	**0.27**	**0.22**	−0.17	−0.18
U10	**0.64***	**0.72***	**0.53**	0.20	−0.01	−0.18

[a]The zonal mean zonal wind anomalies at 70 (U70), 50 (U50), 30 (U30), 20 (U20), and 10 hPa (U10) are used for the QBO indices. The correlations are computed for each season: December to February (DJF), March to May (MAM), June to August (JJA), and September to November (SON), along with an extended winter months from November to March (NDJFM). To remove the impact of the ENSO, correlations are also calculated for DJF excluding the ENSO years (denoted as DJF-). The values that exceed the 95% a priori (a posteriori) confidence level are marked in bold (by an asterisk).

2.2. MJO Index

To investigate the MJO, the outgoing longwave radiation (OLR)-based MJO index (OMI), obtained from the NOAA Earth System Research Laboratory website (http://www.esrl.noaa.gov/psd/mjo/mjoindex/), is used in this study (Figure 1b). Briefly, the principal component time series (PC_1 and PC_2) of the OMI are constructed by projecting the 20–96 day band-pass-filtered OLR onto the two leading empirical orthogonal functions (EOFs) of the 30–96 day eastward filtered OLR [*Kiladis et al.*, 2014]. The monthly mean OMI amplitude is computed by averaging daily amplitude, $\sqrt{PC_1^2 + PC_2^2}$, for each month.

Two additional MJO indices which are commonly used in the literature are also considered. One is the Real-time Multivariate MJO index (RMM) [*Wheeler and Hendon*, 2004], which is obtained from the Australian Bureau of Meteorology website (http://www.bom.gov.au/climate/mjo/). The RMM utilizes 200 and 850 hPa zonal winds, as well as the OLR, averaged over a tropical band (15°S–15°N), to form the two leading EOFs (Table S1 in the supporting information). It has been documented that the OMI is well correlated with the RMM but better traces the convective signal of the MJO, which is our primary interest, than does the RMM [*Kiladis et al.*, 2014]. We also adopt the diagnostics suggested by the U.S. CLIVAR MJO Working Group [*Waliser et al.*, 2009] and derive an MJO index from two leading combined EOFs of the same three, but 20–100 day, band-pass-filtered variables averaged over the tropical band (15°S–15°N). This index, which is similarly defined as the RMM index except for time filtering, is denoted as the working group MJO index (Table S2).

2.3. ENSO Index

The UK Met Office (http://www.metoffice.gov.uk/hadobs/hadisst/) Hadley Centre's sea surface temperature (SST) data set [*Rayner et al.*, 2003] is used to calculate the ENSO indices (Figure 1c). The SST anomalies, obtained as deviations from the monthly climatology, are taken as 3 month running averages. Area averages are then taken for the Niño 3.4 region (170°W–120°W, 5°N–5°S).

3. Negative Relationship Between the QBO and the MJO

To identify the possible impacts of the QBO on MJO activities, we first examine the seasonal Pearson's correlations (R) between the QBO (U50) index and the MJO (OMI) amplitude for various seasons. Estimates of the statistical significance are obtained by applying a two-tailed t test at the 95% confidence level under the null hypothesis that the two time series are uncorrelated. To calculate the t statistic ($= R\sqrt{(N-2)/(1-R^2)}$), the number of seasons (i.e., 33) is used as the degrees of freedom (N) of the time series. Because there is no a priori reason to expect correlations between the time series, we examine the stricter a posteriori confidence levels [*Madden and Julian*, 1971], which in our study roughly corresponds to the 99.85% a priori confidence level.

Significant correlations of −0.59 and −0.49 are observed during the DJF and the extended winter (November–March (NDJFM)), respectively (Table 1 and see also Figure S1). The same relation can be deduced using the zonal wind anomaly at 70 hPa (U70). This negative correlation indicates that MJO activity tends to weaken when the zonal wind in the lower stratosphere is anomalously positive and vice versa. In other words, during the WQBO, MJO amplitude is generally weaker than normal, while it is stronger than normal during the EQBO in the lower stratosphere. Positive correlations of MJO amplitude with zonal winds at 20 and 10 hPa (U20 and U10, respectively) and weaker negative correlations with the zonal wind at 30 hPa (U30) also suggest essentially the same result, considering a time lag of a few months for wind anomalies of the upper stratosphere to propagate down to the lower stratosphere [*Baldwin et al.*, 2001].

It is important to note that the QBO-MJO relationship is evident with other MJO indices (Tables S1 and S2). In addition, the same result holds when ENSO years are excluded (denoted by DJF- in Tables 1, S1, and S2). These results indicate that the stratosphere-troposphere coupling associated with the QBO and MJO is quite robust.

However, it is interesting to find that the QBO-MJO link appears mainly in the boreal winter (Tables 1, S1, and S2). This seasonal dependency is likely associated with the seasonality of the MJO itself because the QBO stays centered at the equator in all seasons and its variance does not change much with seasons. One can speculate that the latitudinal location of MJO activity may play a role for the seasonality of QBO-MJO link. However, it is
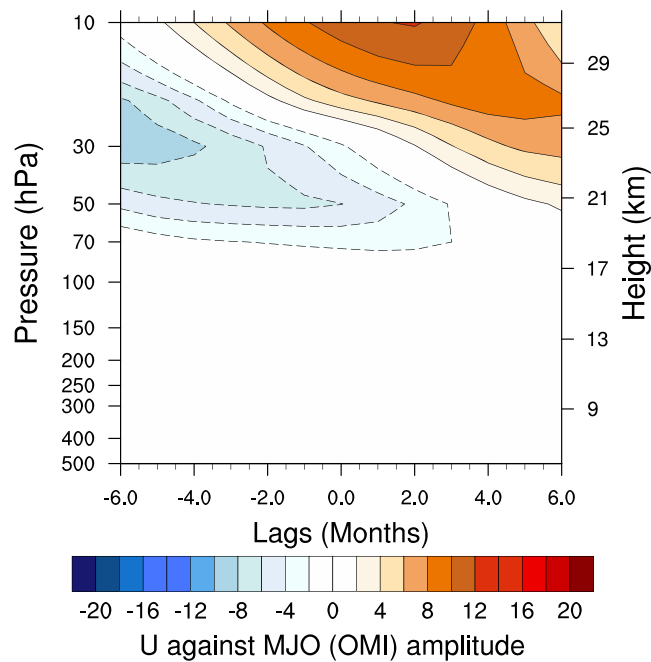
Figure 2. Lead-lagged regression coefficient of equatorial zonal wind (10°S–10°N) against the DJF-mean OMI amplitude is shown. The zonal mean zonal wind is smoothed by applying 3 month running average. Positive lag indicates that OMI is leading zonal wind.

September–November (SON) and March–May (MAM) when MJO convection is aligned well along the equator as in QBO. During DJF, the largest variance of the MJO is located in the Southern Hemisphere subtropics [see *Roundy and Frank*, 2004, Figure 13]. Likewise, during JJA, the MJO activity is centered in the Northern Hemisphere subtropics. Here it is notable that the MJO tends to propagate northward, instead of eastward, during the boreal summer, which may reduce interactions between the MJO and the QBO. The robust QBO-MJO link in the boreal winter is instead likely associated with the MJO amplitude. The amplitude of the MJO peaks during the boreal winter, which may strengthen the MJO response to the QBO. Further studies are required to better understand the seasonality of the QBO-MJO connection.

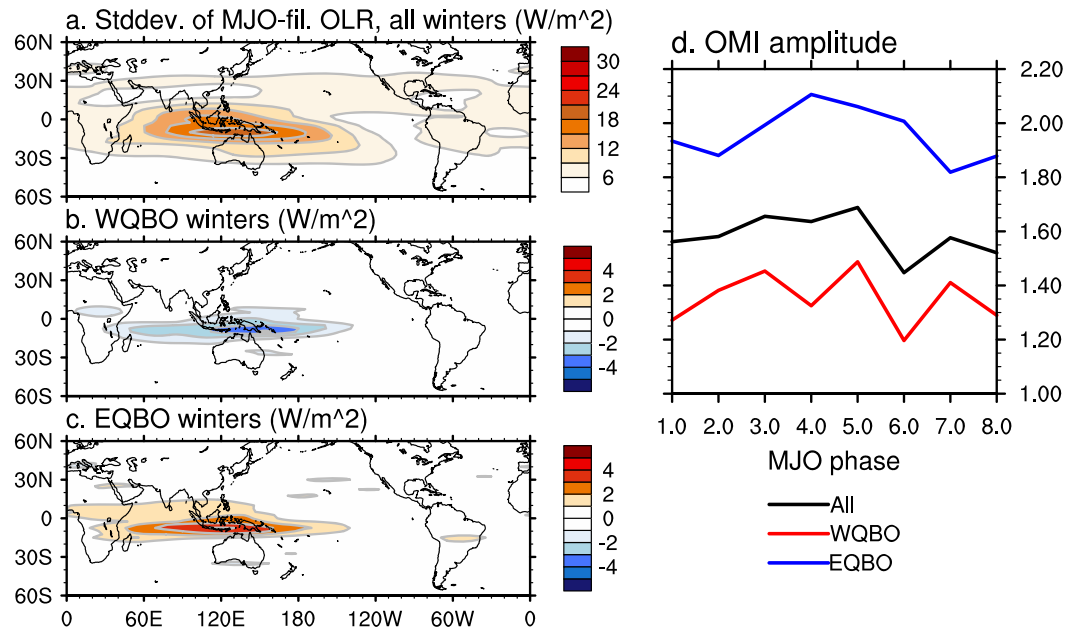For the lead-lag relationship between the QBO and the MJO, because the QBO operates at relatively longer time scales compared to the MJO, it is tempting to think that the stratospheric quasi-biennial signal leads to the changes in intraseasonal convections. This lead-lag relationship can be shown by regressing equatorially averaged (10°S–10°N) zonal wind against the DJF-mean OMI amplitude (Figure 2). Here as for the QBO index, we smooth the monthly zonal mean zonal wind by applying a 3 month running average. On lag month 0 (e.g., DJF U50 versus DJF OMI amplitude), large and negative (positive) regression coefficients can be seen at 50 hPa (10 hPa). This is consistent with the correlation result shown in Table 1. Although the correlation coefficient at lag month −1 (e.g., NDJ U50 versus DJF OMI amplitude) is comparable to the one at lag month 0 (Tables S3), significant negative values at 50 hPa prior to lag month 0 in Figure 2 suggest that an EQBO anomaly tends to precede the strengthening of the MJO.

To examine the spatial changes of the MJO in response to the QBO, we apply MJO filtering [*Wheeler and Kiladis*, 1999] to OLR and then calculate its standard deviation for DJF (Figure 3 and see also Figure S2 for non-ENSO years). Specifically, we first calculate daily OLR anomaly, where the anomaly is a deviation from the climatological mean for each calendar day. The OLR anomaly is then Fourier transformed at each latitudes. When the inverse Fourier transform is reapplied to time and grid space, we retain variability corresponding only to eastward propagating wave numbers 1–5 and 20–100 day periods [*Wheeler and Kiladis*, 1999]. Please note that while the correlation results are obtained regardless of the strength of the QBO, here we make composites for QBO phases, which are defined when the U50 exceeds the half of its standard deviation.

The MJO-filtered OLR variability indicates that MJO activity is centered near 120°E and extends over the region with warm sea surface temperatures (SSTs) (Figure 3a). Supporting the correlation result (Table 1), the standard deviation subsides during the WQBO (Figure 3b) and intensifies during the EQBO (Figure 3c). The QBO-related MJO anomalies range roughly ±10% of the climatology. However, no obvious changes in spatial patterns are observed. The resulting anomalies along 5°S simply represent a strengthening or weakening of MJO convections in the regions where the MJO is climatologically active. But it is notable that they are zonally symmetric (Figures 3b and 3c) as for the QBO-induced mean flow changes in the tropical upper troposphere and lower stratosphere (UTLS) [*Baldwin et al.*, 2001], which probably is an important clue for the QBO-MJO connection. This zonal symmetry contrasts with the ENSO-related MJO activity change. For

Figure 3. (a) The standard deviation of wintertime MJO-filtered OLR for all winters is shown, where the MJO filtering retrieves eastward propagating wave numbers 1–5 and periods 20–100 days. (b, c) As in Figure 3a but for the anomalies for the WQBO (EQBO) winters, respectively. (d) OMI amplitude composites are taken for eight MJO phases of all (black), WQBO (red), and EQBO (blue) winters for active MJO.

example, a few studies have reported an eastward displacement of the MJO activity when El Niño is strong [*Gualdi et al.*, 1999; *Hendon et al.*, 1999, 2007].

Figures 3a–3c are based on all winter days, irrespective of the presence of an active MJO event. In Figure 3d, we perform a composite of the OMI amplitude by detecting only active MJO days for each MJO phase during DJF. The periods of active MJO are identified by using the following conditions: (1) the OMI amplitude must be greater than 1; (2) phase must increase in numerical order, with the exception from phases 8 to 1; and (3) such periods must last longer than 30 days, while MJO does not remain in one particular phase for more than 20 days [*L'Heureux and Higgins*, 2008; *Yoo et al.*, 2014].

A clear separation between the two phases of the QBO is shown in Figure 3d, further validating the negative correlation between the lower stratospheric zonal wind and MJO amplitude. MJO amplitude averaged for all MJO phases during the EQBO is 1.96, which is significantly stronger than that for all years (1.58) and than that for the WQBO (1.35) at the 95% confidence level under the null hypothesis that the difference between the populations is zero.

How does the QBO modulate the organized deep convection in the tropics? It has been proposed that the QBO can affect monthly or seasonal mean tropical convection by modifying the vertical wind shear and/or thermal stratification in the tropical UTLS [*Gray et al.*, 1992; *Giorgetta et al.*, 1999]. A downward propagation of the zonal wind anomaly associated with the WQBO increases the vertical wind shear in the UTLS over the warm pool sector (Figure S3a). Secondary circulation then causes adiabatic warming in the tropical UTLS [*Baldwin et al.*, 2001] and lowers the height of the tropopause [*Reid and Gage*, 1985; *Gray et al.*, 1992], increasing thermal stratification across the tropical tropopause (Figure S3b). If tropical deep convection is influenced by vertical wind shear and thermal stratification in the UTLS [*Nie and Sobel*, 2015], these mean flow changes during the WQBO may provide a less favorable condition for deep convection. The opposite would be true for the EQBO.

The above mechanism appears to operate for the QBO-MJO connection, as the MJO amplitude is negatively correlated with the background absolute vertical wind shear and static stability in the UTLS (Figure 4). Here absolute wind shear is computed by U50 minus U150 averaged over the warm pool section. Likewise, static stability, $-T\frac{d\ln\theta}{dp}$, is calculated over the same area at 100 hPa. A recent study used a cloud-resolving model to
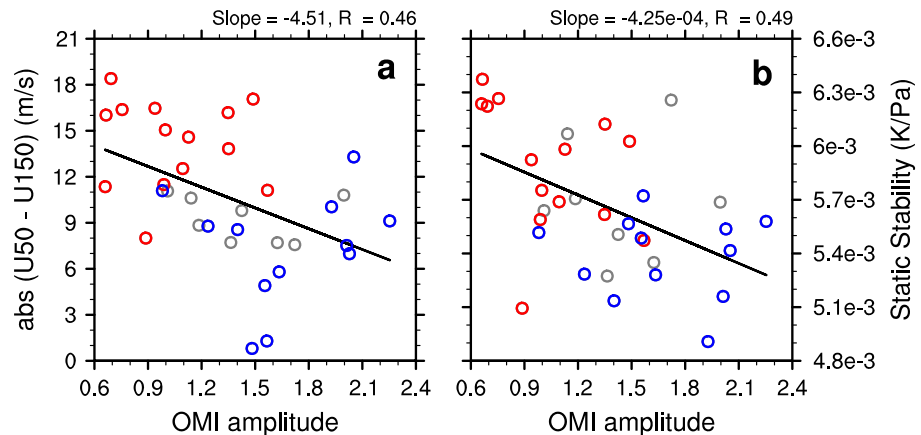
Figure 4. (a) A scatterplot of the zonal wind shear between 50 hPa minus 150 hPa over the tropical warm pool (10°S–10°N, 60°E–180°) and the OMI amplitude, both averaged for DJF. (b) Same as Figure 4a except for the static stability at 100 hPa and the OMI. Red (blue) circles indicate WQBO (EQBO) winters. The black line denotes the regression line of the two variables. Correlation coefficients are indicated at the upper right corner of each figure.

show that the influence of the QBO is carried out through the interactions between large-scale motion, cloud radiative forcing, and convective mass flux [*Nie and Sobel*, 2015]. This is likely the pathway for the MJO convections as well because the cloud-radiation feedback plays a crucial role in MJO dynamics [*Andersen and Kuang*, 2011; *Chikira and Sugiyama*, 2013; *Sobel et al.*, 2014; *Kim et al.*, 2015]. However, it is questionable how effectively the UTLS processes modify the organized deep convection. Further studies, using both observations and numerical models, are required to investigate the detailed processes.

4. Discussion

The present study shows that the boreal winter MJO amplitude greatly varies from year to year over the entire warm pool region depending on QBO phase. Despite the improvement in MJO theory and dynamical prediction, the current generation of climate models does not produce skillful MJO predictions yet, while the MJO is potentially much more predictable [*Neena et al.*, 2014]. Our result suggests that MJO prediction skill could be improved by considering the stratospheric mean state. In fact, by analyzing long-term hindcast simulations of the operational seasonal prediction model, A. G. Marshall et al. (Impact of the Quasi-Biennial Oscillation on prediction of the Madden-Julian Oscillation, submitted to *Geophysical Research Letters*, 2016) showed an enhanced MJO prediction skill during the EQBO winters. Although it needs to be further confirmed by other models that resolve stratospheric processes, this result suggests that the stratospheric data assimilation is crucial for seasonal prediction of the MJO. In this regard, it is also anticipated that statistical prediction of MJO could be improved by taking QBO into account as a potential predictor.

References

Albers, J. R., et al. (2016), Tropical upper tropospheric potential vorticity intrusions during sudden stratospheric warmings, *J. Atmos. Sci.*, in press.

Andersen, J. A., and Z. Kuang (2011), Moist static energy budget of MJO-like disturbances in the atmosphere of a zonally symmetric aquaplanet, *J. Clim.*, *25*(8), 2782–2804, doi:10.1175/JCLI-D-11-00168.1.

Baldwin, M. P., et al. (2001), The quasi-biennial oscillation, *Rev. Geophys.*, *39*(2), 179–229, doi:10.1029/1999RG000073.

Chikira, M., and M. Sugiyama (2013), Eastward-propagating intraseasonal oscillation represented by Chikira–Sugiyama cumulus parameterization. Part I: Comparison with observation and reanalysis, *J. Atmos. Sci.*, *70*(12), 3920–3939, doi:10.1175/JAS-D-13-034.1.

Claud, C., and P. Terray (2007), Revisiting the possible links between the quasi-biennial oscillation and the Indian summer monsoon using NCEP R-2 and CMAP fields, *J. Clim.*, *20*(5), 773–787, doi:10.1175/JCLI4034.1.

Collimore, C. C., D. W. Martin, M. H. Hitchman, A. Huesmann, and D. E. Waliser (2003), On the relationship between the QBO and tropical deep convection, *J. Clim.*, *16*(15), 2552–2568.

Dee, D. P., et al. (2011), The ERA-Interim reanalysis: Configuration and performance of the data assimilation system, *Q. J. R. Meteorol. Soc.*, *137*(656), 553–597, doi:10.1002/qj.828.

Feng, J., P. Liu, W. Chen, and X. Wang (2015), Contrasting Madden–Julian Oscillation activity during various stages of EP and CP El Niños, *Atmos. Sci. Lett.*, *16*(1), 32–37, doi:10.1002/asl2.516.

Garfinkel, C. I., and D. L. Hartmann (2011), The influence of the quasi-biennial oscillation on the troposphere in winter in a hierarchy of models. Part I: Simplified dry GCMs, *J. Atmos. Sci.*, *68*(6), 1273–1289, doi:10.1175/2011JAS3665.1.

Garfinkel, C. I., S. B. Feldstein, D. Waugh, C. Yoo, and S. Lee (2012), Observed connection between stratospheric sudden warmings and the Madden-Julian Oscillation, *Geophys. Res. Lett.*, *39*, L18807, doi:10.1029/2012GL053144.

Giorgetta, M. A., L. Bengtsson, and K. Arpe (1999), An investigation of QBO signals in the east Asian and Indian monsoon in GCM experiments, *Clim. Dyn.*, *15*(6), 435–450, doi:10.1007/s003820050292.

Gottschalck, J., et al. (2010), A framework for assessing operational Madden–Julian oscillation forecasts: A CLIVAR MJO working group project, *Bull. Am. Meteorol. Soc.*, *91*(9), 1247–1258, doi:10.1175/2010BAMS2816.1.

Gray, W. M., J. D. Sheaffer, and J. A. Knaff (1992), Hypothesized mechanism for stratospheric QBO influence on ENSO variability, *Geophys. Res. Lett.*, *19*(2), 107–110, doi:10.1029/91GL02950.

Gualdi, S., A. Navarra, and G. Tinarelli (1999), The interannual variability of the Madden–Julian Oscillation in an ensemble of GCM simulations, *Clim. Dyn.*, *15*(9), 643–658, doi:10.1007/s003820050307.

Gushchina, D., and B. Dewitte (2012), Intraseasonal tropical atmospheric variability associated with the two flavors of El Niño, *Mon. Weather Rev.*, *140*(11), 3669–3681, doi:10.1175/MWR-D-11-00267.1.

Hendon, H. H., C. Zhang, and J. D. Glick (1999), Interannual variation of the Madden–Julian oscillation during austral summer, *J. Clim.*, *12*(8), 2538–2550.

Hendon, H. H., M. C. Wheeler, and C. Zhang (2007), Seasonal dependence of the MJO–ENSO relationship, *J. Clim.*, *20*(3), 531–543, doi:10.1175/JCLI4003.1.

Huang, B., Z.-Z. Hu, J. Kinter III, Z. Wu, and A. Kumar (2012), Connection of stratospheric QBO with global atmospheric general circulation and tropical SST. Part I: Methodology and composite life cycle, *Clim. Dyn.*, *38*(1–2), 1–23, doi:10.1007/s00382-011-1250-7.

Kane, R. P. (1995), Quasi-biennial and quasi-triennial oscillations in the summer monsoon rainfall of the meteorological subdivisions of India, *Mon. Weather Rev.*, *123*(4), 1178–1184.

Kiladis, G. N., et al. (2014), A comparison of OLR and circulation-based indices for tracking the MJO, *Mon. Weather Rev.*, *142*(5), 1697–1715, doi:10.1175/MWR-D-13-00301.1.

Kim, D., M.-S. Ahn, I.-S. Kang, and A. D. Del Genio (2015), Role of longwave cloud–radiation feedback in the simulation of the Madden–Julian Oscillation, *J. Clim.*, *28*(17), 6979–6994, doi:10.1175/JCLI-D-14-00767.1.

Lau, W. K. M., and D. E. Waliser (2005), *Intraseasonal Variability in the Atmosphere-Ocean Climate System*, Springer, Berlin.

L'Heureux, M. L., and R. W. Higgins (2008), Boreal winter links between the Madden-Julian oscillation and the Arctic Oscillation, *J. Clim.*, *21*(12), 3040–3050, doi:10.1175/2007JCLI1955.1.

Lin, H., G. Brunet, and B. Yu (2015), Interannual variability of the Madden-Julian Oscillation and its impact on the North Atlantic Oscillation in the boreal winter, *Geophys. Res. Lett.*, *42*, 5571–5576, doi:10.1002/2015GL064547.

Liu, C., B. Tian, K.-F. Li, G. L. Manney, N. J. Livesey, Y. L. Yung, and D. E. Waliser (2014), Northern Hemisphere mid-winter vortex-displacement and vortex-split stratospheric sudden warmings: Influence of the Madden-Julian Oscillation and Quasi-Biennial Oscillation, *J. Geophys. Res. Atmos.*, *119*, 12,599–12,620, doi:10.1002/2014JD021876.

Madden, R. A., and P. R. Julian (1971), Detection of a 40–50 day oscillation in the zonal wind in the tropical Pacific, *J. Atmos. Sci.*, *28*(5), 702–708.

Madden, R. A., and P. R. Julian (1994), Observations of the 40–50-day tropical oscillation—A review, *Mon. Weather Rev.*, *122*(5), 814–837.

Miura, H., M. Satoh, T. Nasuno, A. T. Noda, and K. Oouchi (2007), A Madden-Julian oscillation event realistically simulated by a global cloud-resolving model, *Science*, *318*(5857), 1763–1765, doi:10.1126/science.1148443.

Miyakawa, T., et al. (2014), Madden–Julian Oscillation prediction skill of a new-generation global model demonstrated using a supercomputer, *Nat. Commun.*, *5*, doi:10.1038/ncomms4769.

Neena, J. M., J. Y. Lee, D. Waliser, B. Wang, and X. Jiang (2014), Predictability of the Madden–Julian Oscillation in the Intraseasonal Variability Hindcast Experiment (ISVHE), *J. Clim.*, *27*(12), 4531–4543, doi:10.1175/JCLI-D-13-00624.1.

Nie, J., and A. H. Sobel (2015), Responses of tropical deep convection to the QBO: Cloud-resolving simulations, *J. Atmos. Sci.*, early online release, doi:10.1175/JAS-D-15-0035.1.

Rayner, N. A., et al. (2003), Global analyses of sea surface temperature, sea ice, and night marine air temperature since the late nineteenth century, *J. Geophys. Res.*, *108*(D14), 4407, doi:10.1029/2002JD002670.

Reid, G. C., and K. S. Gage (1985), Interannual variations in the height of the tropical tropopause, *J. Geophys. Res.*, *90*(D3), 5629–5635, doi:10.1029/JD090iD03p05629.

Roundy, P. E., and W. M. Frank (2004), A climatology of waves in the equatorial region, *J. Atmos. Sci.*, *61*(17), 2105–2132.

Slingo, J. M., D. P. Rowell, K. R. Sperber, and F. Nortley (1999), On the predictability of the interannual behaviour of the Madden-Julian oscillation and its relationship with El Niño, *Q. J. R. Meteorol. Soc.*, *125*(554), 583–609, doi:10.1002/qj.49712555411.

Sobel, A., S. Wang, and D. Kim (2014), Moist static energy budget of the MJO during DYNAMO, *J. Atmos. Sci.*, *71*(11), 4276–4291, doi:10.1175/JAS-D-14-0052.1.

Waliser, D., et al. (2009), MJO simulation diagnostics, *J. Clim.*, *22*(11), 3006–3030, doi:10.1175/2008JCLI2731.1.

Waliser, D. E., K. M. Lau, W. Stern, and C. Jones (2003), Potential predictability of the Madden–Julian Oscillation, *Bull. Am. Meteorol. Soc.*, *84*(1), 33–50, doi:10.1175/BAMS-84-1-33.

Wheeler, M. C., and H. H. Hendon (2004), An all-season Real-time Multivariate MJO index: Development of an index for monitoring and prediction, *Mon. Weather Rev.*, *132*(8), 1917–1932.

Wheeler, M., and G. N. Kiladis (1999), Convectively coupled equatorial waves: Analysis of clouds and temperature in the wavenumber-frequency domain, *J. Atmos. Sci.*, *56*(3), 374–399.

Yoo, C., S. B. Feldstein, and S. Lee (2014), The prominence of a tropical convective signal in the wintertime Arctic temperature, *Atmos. Sci. Lett.*, *15*, 7–12, doi:10.1002/asl2.455.

Zhang, C. (2014), Madden–Julian Oscillation: Bridging weather and climate, *Bull. Am. Meteorol. Soc.*, *94*(12), 1849–1870, doi:10.1175/BAMS-D-12-00026.1.